



Thermal Analysis of a Fluid Inside a Cubicle Surrounded by Peltier Modules

Lakshmanan S¹, Raghunath T¹, Karthik K¹, Bhuvaneswari S^{2,*}, Venkatesan M^{1,*}

¹ School of Mechanical Engineering, SASTRA Deemed University, Tirumalaisamudram, Thanjavur 613 401, Tamilnadu, India.

² Department of Computer Science and Engineering, Srinivasa Ramanujan Centre, SASTRA Deemed University, Kumbakonam 612 001, Tamilnadu, India.

ARTICLE INFO

2025, vol. 45, no.1, pp. 1-9
©2025 TIBTD Online.
doi: 10.47480/isibted.1485008

Research Article

Received: 17 May 2024

Accepted: 22 October 2024

* Corresponding Authors

e-mail: mvenkat@mech.sastra.edu
s.bhuvana@src.sastra.edu

Keywords:

Thermoelectric effect
Peltier module
Machine learning

ORCID Numbers in author order:

0009-0005-2227-2343
0009-0005-5770-5161
0009-0008-3774-9222
0000-0002-3182-7823
0000-0002-6513-7556

ABSTRACT

Peltier modules are thermoelectric devices that convert electric energy to thermal energy. The cost of the cooling process by the module depends on the size of the module. The number of modules is vital in deciding the system's performance. A Peltier module has a high value of the coefficient of performance (COP) for the applied electrical power. The module finds many applications because of its compact size, eco-friendly nature, high durability, noise and vibration-free operation, and low maintenance. Despite these advantages, the Peltier module faces constraints for large-scale applications. This work presents a computational analysis of the temperature distribution of a fluid volume surrounded by four Peltier modules using COMSOL Multiphysics software. Nine different cuboids with multiple Peltier modules are analyzed. The temperature distribution as a function of time is presented. A Machine learning algorithm is developed to predict the temperature of the fluid for varying cuboid sizes surrounded by Peltier modules. The developed machine learning model can predict the average temperature of the fluid domain with an accuracy of 97% for any given Peltier size, fluid volume, applied current, and time.

Peltier Modülleriyle Çevreli Bir Küpün İçindeki Akışkanın Termal Analizi

MAKALE BİLGİSİ

Anahtar Kelimeler:

Termoelektrik etki
Peltier modülü
Makine öğrenimi

ÖZET

Peltier modülleri, elektrik enerjisini termal enerjiye dönüştüren termoelektrik cihazlardır. Modül tarafından gerçekleştirilen soğutma işleminin maliyeti, modülün boyutuna bağlıdır. Modül sayısı, sistemin performansına karar vermede hayati bir rol oynar. Bir Peltier modülü, uygulanan elektrik gücü için yüksek bir performans katsayısı (COP) değerine sahiptir. Modül, kompakt boyutu, çevre dostu yapısı, yüksek dayanıklılığı, gürültüsüz ve titreşimsiz çalışması ve daha az bakım gerektirmesi nedeniyle birçok uygulama bulmaktadır. Bu avantajlara rağmen, Peltier modülü büyük ölçekli uygulamalar için kısıtlamalarla karşı karşıyadır. Bu çalışma, COMSOL Multiphysics yazılımını kullanarak dört Peltier modülüyle çevreli bir sıvı hacminin sıcaklık dağılımının hesaplamalı analizini sunmaktadır. Birden fazla Peltier modülüne sahip dokuz farklı küboid analiz edilmiştir. Sıcaklık dağılımı zamana bağlı olarak sunulmuştur. Peltier modülleriyle çevreli çeşitli küboid boyutları için sıvının sıcaklığını tahmin etmek üzere bir Makine Öğrenmesi algoritması geliştirilmiştir. Geliştirilen makine öğrenmesi modeli, herhangi bir Peltier boyutu, sıvı hacmi, uygulanan akım ve zaman için sıvı alanının ortalama sıcaklığını %97 doğrulukla tahmin edebilmektedir.

NOMENCLATURE

a	Coefficient of Absorption	u	Vector-valued field variable
C	Calorific capacity ($J/kg.K$)	V	Voltage / Tension (V)
c	Coefficient of Diffusion	\emptyset	The specific flow of heat sources (W/m^3)
D	Density vector of the electrical flux	Ω	Computational domain
da	Damping term	$\partial\Omega$	Computational domain boundary
E	Electric field	α	Seebeck Coefficient matrix Conservative flux convection coefficient
Ea	Mass matrix (or mass coefficient)	β	Convection coefficient
f	Source term	γ	Conservative flux source term
g	Boundary source term	ε	Matrix of relative permittivity
h	Field variable coefficient in Neumann Boundary condition	λ	Thermal conductivity ($W/m.K$)
h ^T	Transpose of h	μ	Lagrange Multiplier
J	Electric current density vector	π	Matrix of Peltier coefficient
n	Outward unit normal vector on $\partial\Omega$	ρ	Density (kg/m^3)
q	Heat flow vector	σ	Electrical conductivity (S/m)
r	Coefficient in Neumann Boundary condition	φ	Rate of heat production
T	Absolute temperature (K)	$\nabla, \vec{\nabla}$	Gradient, Vectoral Gradient operator

INTRODUCTION

The Peltier effect, discovered by Jean Charles Athanase Peltier in 1834, is a phenomenon in which an electric current flowing through a junction of two different conductive materials causes a temperature difference across the junction. Peltier modules, known as thermoelectric coolers or TECs, utilize this effect to achieve precise and efficient temperature control. The module finds applications including green buildings, air coolers, Light emitting diode (LED) cooling, polymerase chain reaction (PNA), small-scale refrigerators, and mini/micro heat exchangers. Various works have been reported in the literature related to the analysis of thermal characteristics of Peltier Modules.

Zaferani et al., (2021) discussed the various applications of Peltier cells in aviation and the military using advanced materials like polymers and fibers. The applications include preparing flexible compounds and stretchable electronic devices such as nanogenerators, solar cells, supercapacitors, and carbon nanotube field effect transistors. Antonova and Aparicio et al., (2012) discussed the usage of thermoelectric coolers and calculated the Coefficient of performance. Convective and radiative modes of heat transfer were considered. The temperature sensitivity of the materials was discussed to understand the underlying physics. A tradeoff was found between selecting materials that have suitable electrical conductivity (γ), Seebeck coefficient (α), and thermal conductivity (κ). Seebeck coefficient must be high to have a pronounced Peltier effect. Electrical conductivity must be high to reduce Joule heating, and thermal conductivity must be low to reduce the heat transfer rate. Nasri et al., (2017) discussed the diverse designs of the thermoelectric generators that were flexible and dependent on parameters such as current Intensity and temperature difference. The module performed better with an increase in temperature. The module's energy consumption by cooling the hotter side was also determined. The application of thermoelectric generators in a condensing combi boiler was detailed by Zeki Yilmazoglu et al., (2013). It was concluded that the TEG installation of the combi boiler reduced the electricity consumption. Thermo-electric heating and cooling units were proposed as an alternative for HVAC applications by Zeki Yilmazoglu (2016).

Teffah et al., (2018) discussed using thermoelectric generators as a partial heat sink for the thermoelectric cooler by converting the lost heat into useful energy via the Seebeck effect. The performance of thermoelectric coolers at different input voltages was investigated via simulation and experiments. The results concluded that the electrical potential generation of the thermoelectric generator (TEG) was directly proportional to the input voltage to the thermoelectric cooler (TEC). The thermoelectric module was proposed as a cooling system and an electric power generator. Lyu et al., (2019) studied the thermal behavior of a single-cell battery subjected to different cooling methods, including forced convection using air and liquid cooling. A new design for a cooling system was proposed: a combination of liquid cooling, forced air cooling, and a thermoelectric module. A study was carried out using a hybrid TEC-liquid-air cooling system. The hybrid system showed an improved cooling effect compared to the individual cooling methods in an electric vehicle's battery thermal management system.

Villasevil et al., (2013) modeled a thermoelectric structure with pellets of non-standard geometry and materials. A correlation was proposed based on experiments and a numerical model. Material properties had a direct effect on the thermoelectric devices. For different current values, there was a corresponding shift in the temperature distribution, either above or below, depending upon the polarity of the current, i.e., heating or cooling. Looman (2005) proposed a finite element method to study thermoelectric devices using ANSYS Software. Steady-state and transient-state analyses were conducted in detail for TEGs and TECs. Jaegle (2008) proposed the adoption of thermoelectric multiphysics in the COMSOL Multiphysics library and detailed the governing equations. The temperature is fixed on one side and was commonly adopted in numerical models to quickly visualize the heating/cooling on a side. AB (2008) is a modeling guide used to study the modeling patterns and methods in the COMSOL Multiphysics software. It is used to understand the physical processes in the thermoelectric domain. Venkatesan and Venkataramanan (2020) proposed fixing the hot side temperature for Peltier modules. A fixed incremental value of 5K temperature was used in the study. The temperature difference increased with an increase in current. There was an increased cooling effect with a small

temperature difference and decreased cooling with a very intense hot side for a particular temperature difference.

Recent works report on using soft computing techniques for various thermal applications, including Peltier modules. Zhan et al., (2017) predicted the thermal boundary resistance for thermal management in high-power micro and optoelectronic devices. The concepts of phonon transport of heat transfer and the acoustic and diffuse mismatch models were proposed to calculate the resistance. The Gaussian process regression and Support Vector Regression models (SVRM) gave better results when calculating the regression coefficient. Machine learning models (ML) were suggested as an alternative to the computationally expensive molecular dynamics technique. It was found that the film thickness was one of the critical parameters that affect the thermal film resistance.

Song et al., (2019) proposed using ultrasound to enhance the heat transfer in industrial evaporators. The universal heat transfer coefficient increased by 20%. The most critical controlling variable was the temperature difference between heating steam and evaporation. The prediction used machine learning models. Lower root mean square error was reported by using SVM and NNet algorithms. Qian et al., (2019) predicted the performance of oscillating heat pipes during machining processes. A machine learning model was developed to predict the parameters to dissipate the heat generated during the machining process. Different machine learning algorithms were tested, and the extreme gradient boosting algorithms (XGBoost) performed well. Bassi et al., (2021) developed machine learning models to predict the energy utility of a building accurately. XGBoost, LightGBM, and CatBoost techniques were used to predict the power consumption. The performance characteristics of these algorithms with gradient-boosting regression trees were summarized. It was found that XGBoost was the best algorithm for the considered dataset.

The above literature details the works reported on the Peltier module and the application of soft computing for various related applications. Though Peltier modules have higher COP for lower power supply, their performance for larger-scale applications is limited. The present work attempts to understand the effects of the Peltier module on fluid cooling and heating in varying volumes. A machine learning model is developed to predict the temperature accurately. The specific contribution of parameters (cooling, current, time, Peltier size, and fluid volume) for predicting the output temperature is done with SHAP values. The use of SHAP values by Lundberg & Lee (2017) was derived from Shapley's values based on Shapley's game theory (1953). The application of the machine learning model holds promise in predicting the average temperature of fluid bodies surrounded by large-sized Peltier modules, circumventing the need for computationally intensive simulations. By offering a rapid and reliable means of temperature prediction, the model stands to significantly expedite the design and optimization processes for systems incorporating large Peltier modules. The predicted technique can optimize cooling processes in applications such as electronic device cooling, automotive climate control, medical refrigeration, and industrial equipment thermal management.

PROBLEM DESCRIPTION

In the present work, a fluid is filled in a cubical volume surrounded by four Peltier modules, as shown in Fig. 1(a). Water is considered as the working fluid. The fluid can be heated or cooled by changing the polarity of the Peltier module. A transient analysis is done using the COMSOL Multiphysics package. The variation of the average temperature of the fluid with respect to time is analyzed for different Peltier dimensions, fluid volume, and input current. The current is supplied to one of the highlighted terminals, as shown in Fig. 1(b), while the other terminal is grounded. If the polarity of the supply is reversed, the heating or cooling effect can be changed. One side of the Peltier module is kept constant at 293K, as shown in Figure 1(a). It is assumed that the effect of rising and falling temperature on one side of the module is compensated by providing sufficient external resources, as mentioned in Tefah et al., (2018). It is done to keep the value of temperature difference (ΔT) minimal to obtain the maximum rate of cooling and to maintain adiabatic conditions, as mentioned in (Venkatesan & Venkataramanan (2020), Jaegle (2008) and Nasri et al., (2017)). A detailed parametric study is carried out on the fluid body to find the effect of Peltier dimensions, fluid volume, and input current on the average fluid temperature. Figure 1(b) shows the model setup for Peltier dimension 27x37(mm). A machine learning model is trained with six different Peltier modules of dimensions (in mm) 18x18, 18x27, 27x18, 27x27, 27x37 and 37x27. The model is tested with three datasets, each representing a unique Peltier module data. The testing dataset comprises Peltier modules of dimensions (in mm) 46x46, 56x46, and 46x56.

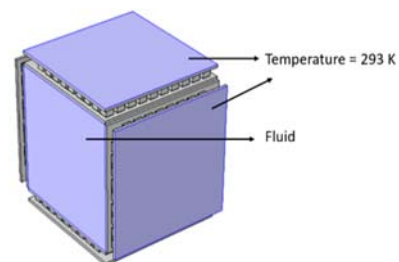


Fig. 1(a). Peltier module of dimension 46x46

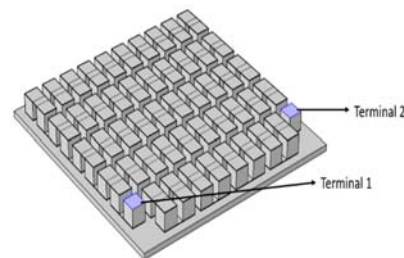


Fig. 1(b). Individual Peltier modules

MESHING AND GRID INDEPENDENCE STUDY

The results shown in Fig. 2 are for a mesh generated for the Peltier module setup of dimension 27 x 27(mm). Studies are carried out starting from extra course mesh to fine mesh elements. A grid independence test is performed to determine the optimal mesh size. The temperature values are supposed to be independent of the mesh size. The model is given a uniform normal meshing. When the number of domain elements exceeds 106841, as shown in Fig. 2, the temperature recorded does not change much. The optimal mesh quality is found to be 0.03556.

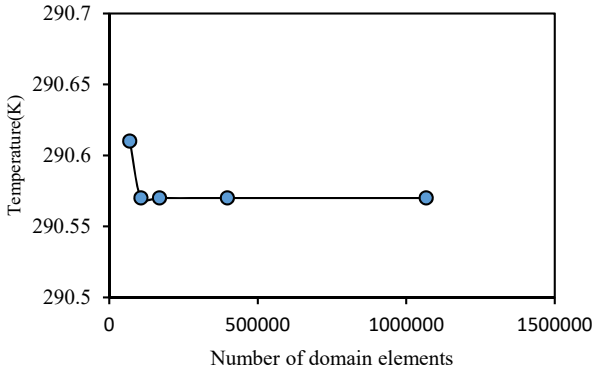


Fig. 2. Grid independence test

GOVERNING EQUATIONS AND BOUNDARY CONDITIONS

These governing equations considering thermoelectric effects and heat transfer for thermoelectric systems are given by Nasri et al., (2017). The Joule effect must be considered for effective modeling of the system. The equations are

$$\rho C \frac{\partial T}{\partial t} + \nabla_q = \phi \quad (1)$$

The equation of continuity of electric charge:

$$\nabla \left[J + \frac{\partial D}{\partial t} \right] = 0 \quad (2)$$

The electric field E can be obtained from an electric scalar potential as detailed in Antonova and Looman (2005) and is as follows:

$$E = -\nabla\phi \quad (3)$$

The thermoelectric constitutive equations from Antonova and Looman (2005) are:

$$q = [\pi]J - [\lambda]\nabla T \quad (4)$$

$$J = [\sigma](E - [\alpha]\nabla T) \quad (5)$$

The constitutive equation for a dielectric medium from Antonova and Looman (2005):

$$D = [\varepsilon]E \quad (6)$$

The coupled heat equation and Poisson's equation are extended by the thermoelectric effects and solved simultaneously to obtain the temperature and Voltage values from Jaegle (2008):

$$-\vec{\nabla} \cdot \left((\sigma\alpha^2 T + \lambda)\vec{\nabla} T + \sigma\alpha T \vec{\nabla} V \right) = \sigma \left((\vec{\nabla} V)^2 + \alpha \vec{\nabla} T \vec{\nabla} V \right) \quad (7)$$

$$\vec{\nabla} \cdot (\sigma\alpha \vec{\nabla} T) + \vec{\nabla} \cdot (\alpha \vec{\nabla} V) = 0 \quad (8)$$

While implemented in the COMSOL Multiphysics interface, the equations can be written as partial differential equations of the variable u (dependent on T and V) in one to three dimensions. The general form of the equation, as detailed in Jaegle (2008) and AB (2008), are

$$e_a \frac{\partial^2 u}{\partial t^2} + d_a \frac{\partial u}{\partial t} + \nabla \cdot (-c\nabla u - \alpha u + \gamma) + \beta \cdot \nabla u + \alpha u = f \text{ in } \Omega \quad (9)$$

$$n \cdot (-c\nabla u - \alpha u + \gamma) + qu = g - h^T \mu \text{ in } \partial\Omega \quad (10)$$

$$hu = r \text{ in } \partial\Omega \quad (11)$$

The first equation in this list is the PDE, which must be solved for thermoelectric systems.

Equation 10 has a Neumann boundary condition that allows for a constant heat flux at the boundary. Equation 11 has a Dirichlet boundary condition in which a constant surface temperature is given.

NUMERICAL MODEL AND VALIDATION

The model has been validated using the data reported by Villasevil et al., (2013). A comparison between numerical values of surface temperature and the results of Villasevil et al., (2013) for different current values is shown in Fig. 3. It is observed that the simulation results follow the same pattern as reported by Villasevil et al., (2013). The temperatures of the present numerical model match well with those of Villasevil et al., (2013) for 1A, 1.5A, and 2A. Further analysis of other cubical volumes is done with the validated numerical model.

RESULTS AND DISCUSSION

Heat transfer characteristics of a single Peltier module

The temperature distribution for nine different Peltier geometries is simulated with varying volumes of fluid and five different current values (1 A, 1.5 A, 2 A, 2.5 A, 3 A). The heating and cooling effects are studied for all the Peltier geometries. The variation of temperature with respect to time follows a parabolic curve where the temperature increases or decreases based on the polarity and reaches a steady state after a specific time. A single Peltier module is modeled, and its temperature distribution is studied. As a further extension, the cubical volume surrounded by four Peltier modules is modeled with a validated numerical model, and further analysis is done.

Surface temperature (Single Peltier module): The variation of surface temperature for a single 46 x 46mm Peltier module at 100s at 2A current for both heating and cooling

are shown in Fig. 4. The surface temperature variation for all the nine single modules is carried out.

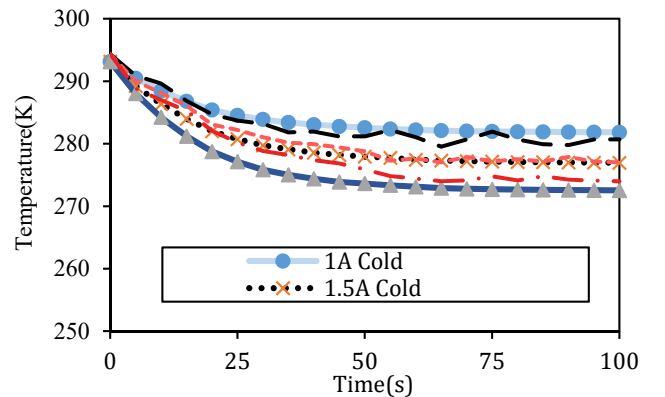


Fig. 3. Comparison of the temp. values with Villasevil et al., (2013)

It can be observed that there is a temperature rise or drop (based on the polarity) initially, and it settles down to a steady-state value depending upon the current and time. A steady temperature distribution is reached after the mentioned time. Different modules require different times to reach the steady temperature distribution, and they are noted for all nine single modules.

Bulk fluid surface temperature distribution: The fluid domain has been introduced, and Peltier modules of varying sizes surround it. The study carried out for the 27 x 27(mm) Peltier setup is shown in Fig. 5 (a), and its bulk surface temperature is also shown. The case is for the supply 1A, and

the fluid surface temperature distribution in the 1800s is shown. Similar studies are done for other modules. Fig. 5(b) shows the transient temperature distribution for a 46 x 46 module at 100s

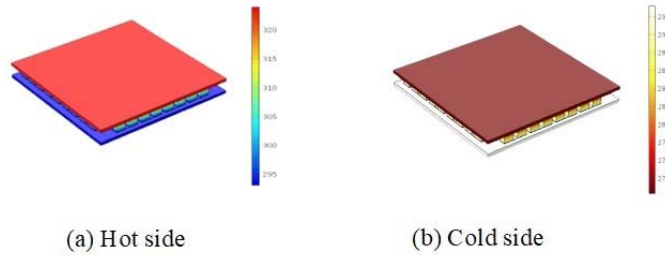


Fig. 4. Surface temperature of module for current value 2 Amps (Time = 100s)

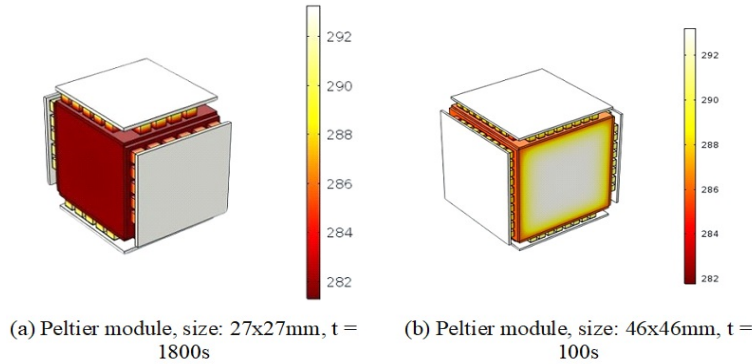


Fig. 5 Surface temperature distribution

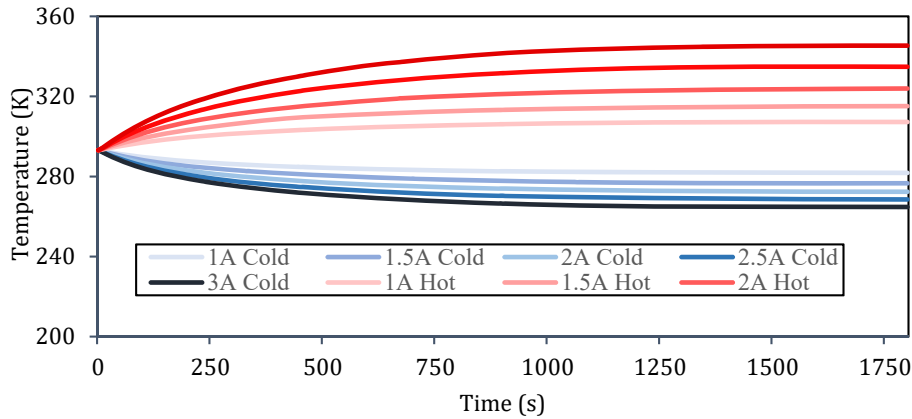


Fig. 6. Variation of Fluid Temperature for different current values (Peltier module, size: 27x27mm)

Bulk fluid surface temperature variation with respect to time at different current values for the Peltier module 27 x 27(mm) has been plotted. It is shown in Fig. 6. Here, the temperature of the fluid increases or decreases based on the polarity and reaches a steady state after some time, depending on the current value. It is to be noted that a steady state has been achieved in all the conditions around 1250s.

Training dataset

The temperature distribution is collected as a function of time for varying Peltier volume and current. The machine learning model is trained with six different Peltier geometries. The remaining three modules are used as test cases. The size of the model varies from 18mm to 46mm. The analysis is done for varying dimensions of length and breadth. The fluid volume depends upon the size of the module. The input current ranges from 1A to 3A, increasing

in steps of 0.5A. Fig. 7 shows the six Peltier modules used to train the model. The parameters used as the input for the machine-learning model are

- (i) length of the Peltier module (in mm),
- (ii) breadth of the Peltier module (in mm),
- (iii) volume of the fluid (in cubic mm),
- (iv) polarity (1 for cooling and 0 for heating),
- (v) input current (in A) and
- (vi) time (in seconds).

Testing dataset

The testing dataset comprises Peltier modules of dimensions 46mm x 46mm, 46mm x 56mm, and 56mm x 46mm, varying from the training dataset's sizes. Input current ranges from 1A to 3A in 0.5A increments, akin to the training dataset. These dimensions ensure diversity, while fluid volume adjusts accordingly. Fig. 8 depicts the three

Peltier modules utilized for testing to evaluate the model's generalization to new dimensions. This dataset aims to assess the generalization capability of the machine learning

model trained on the six Peltier geometries, extending its applicability to previously unseen dimensions.

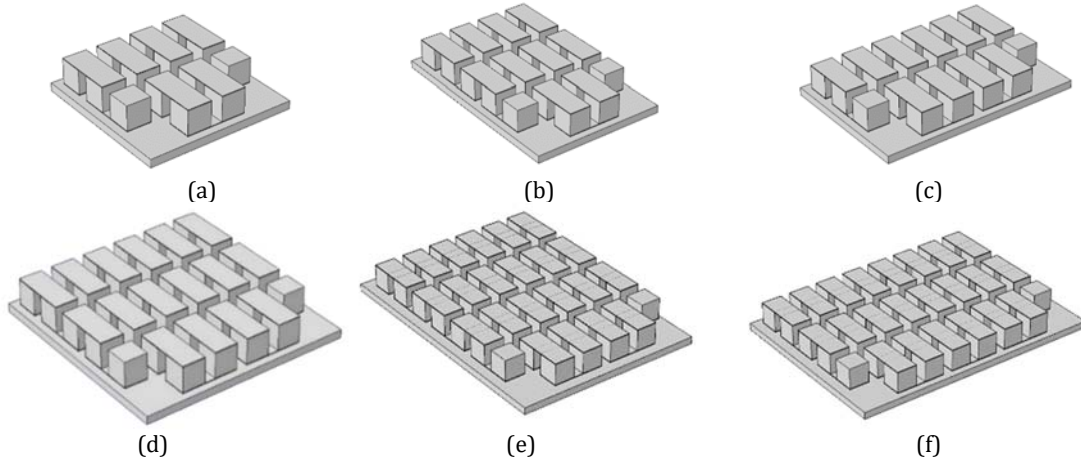


Fig. 7 Peltier module, size: (a) 18x18mm, (b) 18x27mm, (c) 27x18mm, (d) 27x27mm, (e) 27x37mm, (f) 37x27mm

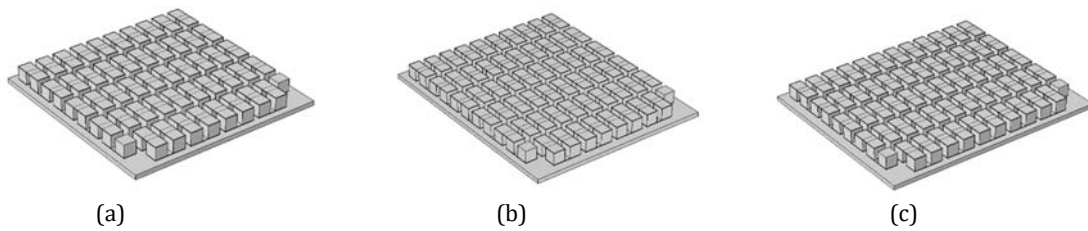


Fig. 8 Peltier module, size: (a) 46x46mm, (b) 46x56mm, (c) 56x46mm

Machine Learning Models

Machine learning algorithms are essential for temperature prediction of varying Peltier modules (Vipin et al., 2024). These algorithms enable prediction and thermal management with nonlinear mapping functions with a fair amount of data. This study examines four popularly demonstrated machine learning models to predict the average temperature of fluid domains at varying Peltier modules. Based on the diverse working nature of the models, Decision Tree, Gradient Boosting, Random Forest, and XGBoost are considered for comparison. Using open-source Python libraries like Scikit-Learn and Keras, the implementation for all four models has been done. The investigation of utilized learning algorithms is given below.

Decision Tree

A decision tree is a visual representation of the cognitive strategies employed in various decision-making processes (Dang et al., 2022). The decision tree has three types of nodes: the root, internal, and leaf nodes. The root nodes initiate the decision-making process, whereas the internal nodes segment the input space into subspaces guided by the discriminant function $f(x)$, which begins at the root.

$$f(x) = W_g(x) + \theta$$

In the neural network, $g(x)$ is the activation function of each neuron, and $f(x)$ is its output function. The decision tree can be categorized into nonlinear and linear based on the form of $g(x)$. Sometimes, an internal node within a decision tree may not necessitate branching to a leaf node. Therefore, these internal nodes are designated leaf nodes if conditions are met. The method employs a local search approach to train decision trees. Nevertheless, this approach may result in local optima and not guarantee global optimization.

Random Forest

In machine learning, Random Forest is an algorithm derived from baseline decision trees. It is designed to overcome the drawbacks using a single decision tree, namely overfitting and instability. Random forest algorithm aims to generate more reliable outcomes by aggregating predictions from multiple decision trees (Carvalho et al., 2019). Additionally, it does not require assumptions regarding the statistical distribution of the data, so it can be utilized even in scenarios where the relationships between variables are non-linear. Each decision tree in the forest has its unique training set generated from the original training dataset using bootstrap sampling in the RF formulation. The final output is constructed by the determining average over predictions of all decision trees:

$$Avg_{RF}(x) = \frac{\sum_{i=1}^N pred(x)}{N}$$

Gradient Boosting

A boosting algorithm is a type of learning algorithm that combines multiple sampler models to fit models. Models used in sampling are usually base models that have been trained using weak or base learners (Park et al., 2023). When a boosting technique is applied, the accuracy of these models is significantly enhanced compared to random guessing. With Gradient Boosting (GB), retrieving importance scores for each feature (attribute) is relatively straightforward. Based on these scores, assessing the significance of boosted decision trees in constructing a model is possible. In order to facilitate the ranking and comparison of attribute values, each feature in the dataset is ranked and compared based on its importance. The importance of a split point in a decision tree is determined based on how many observations are associated with that node. The performance measure can be the purity score or another error function for selecting split points.

XGBoost

A prominent implementation of boosting algorithms is Extreme Gradient Boosting (XGBoost). It is a free and open-source toolkit developed by the Distributed Machine Learning Community (DMLC) and distributed by the DMLC (Gao et al., 2024). It enhances transparency and facilitates straightforward tree visualization, thus fostering a vibrant and engaged community. There are several notable differences between XGBoost and other boosting solutions, including the proportionally shrinking of leaf nodes, the penalization of trees, and adding randomization parameters. As part of an ensemble machine learning framework based on decision trees, the XGBoost uses gradient to construct regression and classification models. This algorithm was developed by Chen et al., (2016) as an efficient implementation of the gradient-boosting methodology. It should be noted that XGBoost offers several advantages over gradient boosting, including more intelligent tree partitioning, shorter leaf nodes, random hidden node generation, and the ability to make predictions outside of the core. As a result of its seamless integration with the Python programming language and its widespread use in Kaggle competitions, the regression method has become increasingly popular in recent years. XGBoost outperformed four prominent machine learning models for predicting fluid domain temperatures across various Peltier modules. The next step may be to conduct sensitivity analyses, tune the parameters, and optimize XGBoost's predictive capabilities. With continuous optimization possibilities, the dynamic nature of machine learning algorithms is highlighted, and the potential of XGBoost in temperature prediction and thermal management for Peltier modules is encouraged. The XGBoost model is used to predict the temperature distribution curves for various combinations of the parameters.

The graph in Fig 9 shows a 56 x 46 module for a 1A current. Similar graphs are obtained for all combinations, and the prediction accuracy is 97%.

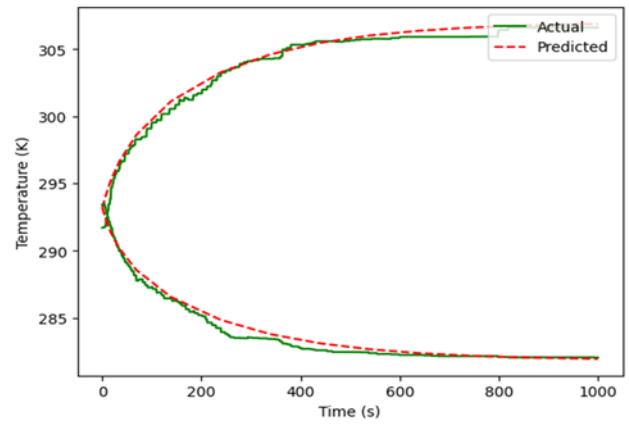


Fig. 9. Comparison between the numerical model and XGBoost model

Model Optimization

This section explains comprehensive insight into the intricacies of the hyperparameter tuning process for machine learning models, namely, XGBoost, Gradient Boosting, Random Forest, and Decision Tree (Cotorogea et al., 2022). These models are implemented to predict the fluid domain's average temperature with varying Peltier module sizes. Bayesian optimization efficiently identifies optimal hyperparameter values by iteratively selecting the most promising parameter configuration. This optimization technique effectively explores the set of hyperparameter spaces to search for optimal values. In selecting hyperparameters, objective functions of Bayesian optimization techniques such as Expected Improvement (EI) and Upper Confidence Bound (UCB) play a significant role in balancing exploration and exploitation of the hyperparameter space. The objective oversees estimating the potential improvement at any given point while evaluating the objective function given its existing state. As the proposed work is evaluated on three datasets, the table below consists of hyperparameters for each machine-learning model with its corresponding optimal values.

Table 1. List of optimal hyperparameter values using Bayesian Optimisation

Datasets	Models with their optimal hyperparameter values
1 st dataset	XGBRegressor (gamma = 1, learning_rate = 0.05, max_depth = 5, min_child_weight = 9, n_estimators=38, reg_alpha=180) GradientBoostingRegressor (learning_rate=0.08, max_depth=4,max_features='sqrt', min_samples_leaf=50, min_samples_split=50,n_estimators=84) RandomForestRegressor (max_depth=6, max_features=0.72, min_samples_leaf=1, min_samples_split=10) DecisionTreeRegressor(max_depth=12,min_samples_split=12,max_leaf_nodes=19, max_features='auto')
2 nd dataset	XGBRegressor (gamma = 8, learning_rate =0.08, max_depth = 5, min_child_weight =5, n_estimators=53, reg_alpha=28) GradientBoostingRegressor (learning_rate= 0.15, max_depth=4, max_features='sqrt', min_samples_leaf=34, min_samples_split=2,n_estimators=75) RandomForestRegressor (max_depth=6, max_features=0.7097968171311817, min_samples_leaf=6, min_samples_split=5) DecisionTreeRegressor (max_depth=5,max_leaf_nodes=20,min_samples_split=20)
3 rd dataset	XGBRegressor(gamma = 8, learning_rate =0.08, max_depth = 5, min_child_weight =5, n_estimators=53, reg_alpha=28) GradientBoostingRegressor (learning_rate= 0.108, max_depth=6, max_features = 'sqrt', min_samples_leaf=8, min_samples_split=2,n_estimators=75) RandomForestRegressor(max_depth=6, max_features=0.721, min_samples_leaf=5, min_samples_split=4) DecisionTreeRegressor(max_depth=5,max_leaf_nodes=20,min_samples_split=6)

RESULTS AND DISCUSSIONS

The proposed machine learning models are implemented in hardware comprising a Windows 11 operating system and an Intel Core i5 processor with 8 GB RAM. The experimentations are performed using Jupyter Notebook, and the models are evaluated in terms of performance

metrics, including accuracy (Acc), Mean Squared Error (MSE), and Mean Absolute Error (MAE). The following sections examine the evaluation of proposed machine learning models for temperature prediction. The experimental findings indicate the performance of each machine learning model with respect to three different datasets.

Performance comparison

Four diverse machine learning models have been chosen to compare the effectiveness of prediction tasks: XGBoost, gradient boosting, random forest, and decision tree.

Table 2 consists of an error metrics comparison over three considered datasets. It is observed that XGboost outperforms all other prediction models with the highest accuracy of 97% when trained on the first dataset, with the lowest average absolute error of 2.04. As XGboost exhibits superior performance, it can be concluded that it is the most suitable temperature prediction model for varying Peltier sizes.

Table 2. Performance comparison of four machine learning models using error metrics

ML models /Error metrics	1 st Dataset			2 nd Dataset			3 rd Dataset		
	Acc	MSE	MAE	Acc	MSE	MAE	Acc	MSE	MAE
XGBoost	0.97	7.65	2.04	0.97	6.5	1.97	0.97	5.60	1.78
Gradient Boosting	0.96	8.01	2.16	0.96	6.9	2.05	0.96	977	2.20
Random Forest	0.94	13.07	2.83	0.95	12.52	2.65	0.95	2.57	12.01
Decision Tree	0.90	22.58	3.64	0.94	13.52	2.58	0.95	2.61	12.15

SHAP analysis

The SHAP (SHapley Additive exPlanations) analysis graphs are concerned with the feature's importance for model prediction. It consists of horizontal bars representing typical feature importance scores; notably, longer bars indicate more significant importance. By observing the direction of the bars, it can be stated that the positive SHAP values contribute towards increasing the model's prediction.

Figure 10 shows the feature-based SHAP analysis of the best-proposed prediction model, XGBoost, for varying Peltier sizes. It is inferred from the graph that the "cooling" feature has longer bars, which is identified as the most influential feature that contributed to accurate predictions.

CONCLUSION

The effect of Peltier modules of varying sizes on cooling and heating fluid is detailed in the study. Peltier parameters such as width, height, input current, polarity, and the volume of the fluid body are varied. A machine learning model has been developed based on the collected data to predict the average temperature of the fluid body. The results show that the XGBoost algorithm predicted the fluid temperature well with an average accuracy of 97% across the three different testing datasets. The present study emphasizes the computational analysis of temperature distribution using COMSOL Multiphysics software. The approach addresses the computational expense of varying module sizes, ensuring accurate and efficient modeling. By developing a machine learning algorithm to predict fluid temperatures, the study highlights significant time savings and enhances the ability to evaluate different configurations quickly. This predictive mechanism reduces the need for extensive computational resources and allows rapid optimization. This ML model serves as a memory map, providing a valuable resource for expanding into other applications involving Peltier modules. The study will help to reduce the overall cost, time, and simulation efforts required to select the appropriate setup for Peltier-based devices. The research contributes to more economically viable and time-efficient solutions in thermoelectric systems by streamlining the evaluation process.

REFERENCES

- AB, C., (2008). COMSOL Multiphysics Modeling Guide.
- Antonova, E. E. & Looman, D. C., (2005). Finite Elements for Thermoelectric Device Analysis in ANSYS. *Canonsburg, USA*. <https://doi.org/10.1109/ICT.2005.1519922>
- Aparicio, J. L. P., Palma, R. & Taylor, R. L., 2012. Finite element analysis and material sensitivity of Peltier thermoelectric cells coolers. *International Journal of Heat and Mass Transfer*, pp. 1363-1374. <https://doi.org/10.1016/j.jheatmasstransfer.2011.08.031>
- Bassi, A., Anika S., Arjun S., Hanna S., Connor G., and Jonathan H. Chan. (2021). Building Energy Consumption Forecasting:

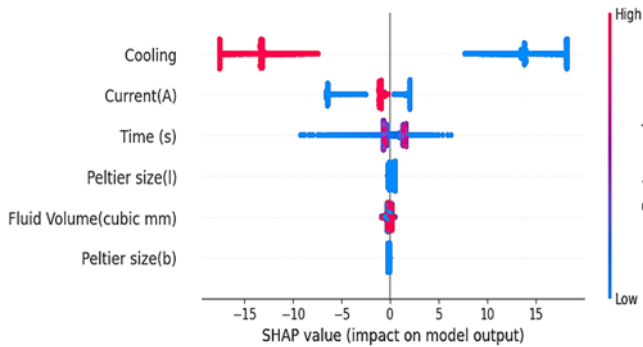


Fig. 10 (a) Illustration of SHAP values for XGBoost model using Peltier size of 46×46

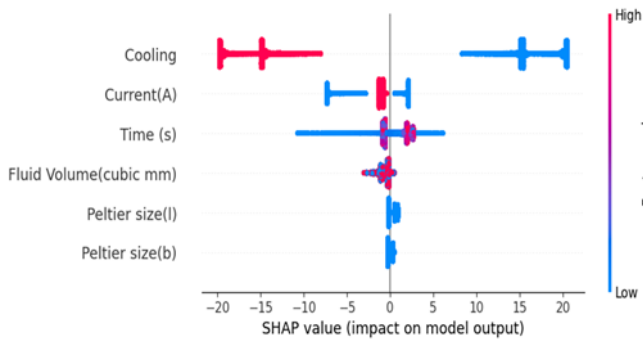


Fig. 10 (b) Illustration of SHAP values for XGBoost model using Peltier size of 56×56

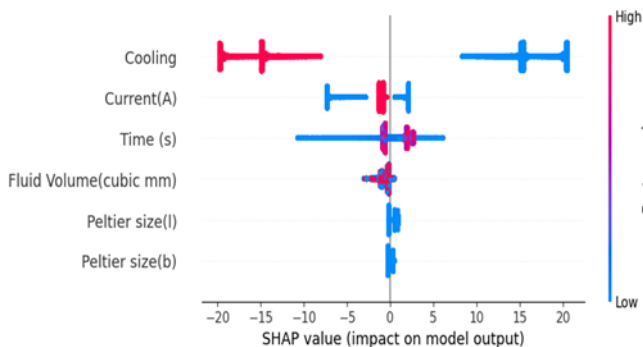


Fig. 10 (c) Illustration of SHAP values for XGBoost model using Peltier size of 46×56

- A Comparison of Gradient Boosting Models. Bangkok, Thailand, 12th International Conference on Advances in Information Technology.
<https://doi.org/10.1145/3468784.3470656>
- Carvalho, T. P., Soares, F. A., Vita, R., Francisco, R. D. P., Basto, J. P., & Alcalá, S. G. (2019). A systematic literature review of machine learning methods applied to predictive maintenance. *Computers & Industrial Engineering*, 137, 106024.
<https://doi.org/10.1016/j.cie.2019.106024>
- Chen, T., Guestrin, C. (2016). Xgboost: A scalable tree boosting system. In *Proceedings of the 22nd acm sigkdd international conference on knowledge discovery and data mining* (pp. 785-794).
<https://doi.org/10.1145/2939672.293978>
- Cotorogea, B. P. F., Marino, G., & Vogl, S. (2022). Data driven health monitoring of Peltier modules using machine-learning-methods. *SLAS technology*, 27(5), 319-326.
<https://doi.org/10.1016/j.slast.2022.07.002>
- Dang, W., Guo, J., Liu, M., Liu, S., Yang, B., Yin, L., & Zheng, W. (2022). A semi-supervised extreme learning machine algorithm based on the new weighted kernel for machine smell. *Applied Sciences*, 12(18), 9213.
<https://doi.org/10.3390/app12189213>
- Gao, X., Zhang, K., Zhang, Z., Wang, M., Zan, T., & Gao, P. (2024). XGBoost-based thermal error prediction and compensation of ball screws. *Proceedings of the Institution of Mechanical Engineers, Part B: Journal of Engineering Manufacture*, 238(1-2), 151-163.
<https://doi.org/10.1177/095440542311571>
- Jaegle, M., 2008. *Multiphysics Simulation of Thermoelectric Systems - Modeling of PeltierCooling and Thermoelectric Generation*. Hannover, s.n.
- Lundberg, S. M. & Lee, S. I., 2017. A unified approach to interpreting model predictions. *Advances in neural information processing systems*, p. 30.
<https://doi.org/10.48550/arXiv.1705.07874>
- Lyu Y, Siddique A.R.M, Majid S.H., Biglarbegian M, Gadsden S.A., Mahmud S., (2019). Electric vehicle battery thermal management system with thermoelectric cooling. *Energy Reports*, 5, 822-827.
<https://doi.org/10.1016/j.egy.2019.06.016>
- Nasri W, Djebali R, Dhaoui S, Abboudi S, Kharroubi H, (2017). Finite Elements Multiphysics Investigation of Thermoelectric Systems for Electricity and Cooling Generation. *International Journal of Modern Studies in Mechanical Engineering*, 3(4), pp. 1-13.
<http://dx.doi.org/10.20431/2454-9711.0304001>
- Park, H. I., Cho, T. J., Choi, I. G., Rhee, M. S., & Cha, Y. (2023). Object classification system using temperature variation of smart finger device via machine learning. *Sensors and Actuators A: Physical*, 356, 114338.
<https://doi.org/10.1016/j.sna.2023.114338>
- Qian N, Wang X, Fu Y, Zhao Z, Xu J, Chen J, (2019). Predicting heat transfer of oscillating heat pipes for machining processes based on extreme gradient boosting algorithm. *Applied Thermal Engineering*, 164, 114521.
<https://doi.org/10.1016/j.applthermaleng.2019.114521>
- Shapley, L. (1953) A Value for n-Person Games. In: Kuhn, H. and Tucker, A., Eds., *Contributions to the Theory of Games II*, Princeton University Press, Princeton, 307-317.
<https://doi.org/10.1515/9781400881970-018>
- Song J, Tian W, Xu X, Wang Y, Li Z, (2019). Thermal performance of a novel ultrasonic evaporator based on machine learning algorithms. *Applied Thermal Engineering*, 148, pp. 438-446.
<https://doi.org/10.1016/j.applthermaleng.2018.11.083>
- Teffah, K., Zhang, Y. & Mou, X., (2018). Modeling and Experimentation of New Thermoelectric Cooler-Thermoelectric Generator Module, *Energies*, 11(3), 576.
<https://doi.org/10.3390/en11030576>
- Venkatesan, K. & Venkataramanan, M., (2020). Experimental and Simulation Studies on Thermoelectric Cooler: A Performance Study Approach. *International Journal of Thermophysics*, 41, Article number 38.
<https://doi.org/10.1007/s10765-020-2613-2>
- Villasevil, F., López, A. & Fisac, M., (2013). Modeling and Simulation of a Thermoelectric Structure with Pellets of Non-Standard Geometry and Materials. *International Journal of Refrigeration*, 36 (5), 1570-1575.
<https://doi.org/10.1016/j.jirefrig.2013.02.014>
- Vipin, K. E., & Padhan, P. (2024). Machine-Learning Guided Prediction of Thermoelectric Properties of Topological Insulator Bi₂Te₃-xSex. *Journal of Materials Chemistry C*, 12, 7415-7425.
<https://doi.org/10.1039/D4TC01058B>
- Zaferani, S., Sams, M., Ghomashchi, R. & Chen, Z.-G., (2021). Thermoelectric Coolers as Thermal Management Systems for Medical Applications: Design, Optimization, and Advancement. *Nano Energy*, Volume 90, Part A, 106572
<https://doi.org/10.1016/j.nanoen.2021.106572>
- Zhan, T., Fang, L. & Xu, Y., (2017). Prediction of thermal boundary resistance by the machine learning method. *Scientific Reports*, 7(7109).
<https://doi.org/10.1038/s41598-017-07150-7>
- Zeki Yilmazoglu, M., (2016). Experimental and numerical investigation of a prototype thermoelectric heating and cooling unit, *Energy and Buildings*, 113, 51-60.
<https://doi.org/10.1016/j.enbuild.2015.12.046>
- Zeki Yilmazoglu, M., Salih K., Tamer C., Turgut O. Y., and Senol B., (2013). Experimental Study on Thermoelectric Generator Performance Applied to a Combi Boiler, 13th UK Heat Transfer Conference, UKHTC2013/143, 2 - 3 September 2013, Imperial College London, 143-1-8.